Evaluation of methods for one-dimensional spatial analysis of two-dimensional patterns in mouse chimaeras

Journal of Anatomy

J. Anat. (2011) **219**, pp418–437 doi: 10.1111/j.1469-7580.2011.01395.x

Evaluation of methods for one-dimensional spatial analysis of two-dimensional patterns in mouse chimaeras

Benjamin A. Hodson,[1] Mathieu Unbekandt,[2] Margaret A. Keighren,[1]* Anthea Springbett[3] and John D. West[1]

[1]*Division of Reproductive and Developmental Sciences, Genes and Development Group, University of Edinburgh, George Square, Edinburgh, UK*
[2]*Centre for Integrative Physiology, University of Edinburgh, George Square, Edinburgh, UK*
[3]*Roslin Institute (Edinburgh), Roslin, Midlothian, UK*

Abstract

The relative extent of cell mixing in tissues of mouse chimaeras or mosaics can be studied by comparing the distributions of the two cell populations in the tissues. However, the mean patch size is misleading because it is affected by both the extent of cell mixing and the relative contributions of the two cell populations. Previous work suggested that effects attributable to differences in tissue composition among chimaeras can be factored out either by correcting the mean patch size or by using the median patch size for the minority cell population and restricting the analysis to grossly unbalanced chimaeras. In the present study, computer simulations of two-dimensional mosaic arrays of black and white squares (representing cells) were used to simulate chimaeric tissues. Random arrays simulated tissues with extensive cell mixing, arrays of cell clumps (representing coherent clones) simulated less mixed tissues, and striped arrays simulated tissues with elongated but fragmented descendent clones. The computer simulations predicted that (i) the median patch length (minority cell population) and the corrected mean patch length would both distinguish between random and clumped patterns and (ii) differences in the variation of the composition of two perpendicular series of one-dimensional transects would distinguished between stripes and randomly orientated patches. Both predictions were confirmed by analysis of histological sections of the retinal pigment epithelium from fetal and adult mouse chimaeras. This study demonstrates that two types of non-random two-dimensional variegated patterns (clumps and stripes) can be identified in chimaeras without two-dimensional reconstruction of serial sections.

Key words: chimaera; chimera; computer simulation; eye; mosaic; patch size; retinal pigment epithelium; spatial analysis.

Introduction

Spatial analysis of mosaic or chimaeric tissues, composed of two genetically distinct cell populations, can provide information about cell mixing during organogenesis. The comparison of spatial distributions of cells in different groups of chimaeras requires objective criteria to describe the size, shape and distribution of cells of like genotype in variegated chimaeric tissues. We use the terms patch, coherent clone and descendent clone as previously explained (West et al. 1997). A *patch* is defined as a group of cells of like genotype, which are contiguous at the time of consideration and is a unit that can be measured directly in chimaeric tissue. However, it may comprise one or several neighbouring 'coherent clones' of the same genotype. A *coherent clone* is defined as a group of clonally related cells, which have remained contiguous throughout the history of the embryo (Nesbitt, 1971). A *descendent clone* is any group of clonally related cells irrespective of whether they have remained contiguous throughout development.

The retinal pigment epithelium (RPE) is an epithelial layer that is one cell thick and, in pigmented/albino mosaics or pigmented↔albino chimaeras, the RPE appears as a two-dimensional variegated patchwork of black and white cells

Correspondence
Dr John West, Division of Reproductive and Developmental Sciences, Genes and Development Group, The University of Edinburgh, Hugh Robson Building, George Square, Edinburgh EH8 9XD, UK. T: 0131-650-3112; F: 0131-651-1706; E: John.West@ed.ac.uk
*Present address: MRC Human Genetics Unit, Crewe Road, Edinburgh, EH4 2XU, UK.

Accepted for publication *21 April 2011*
Article published online *27 May 2011*

(Tarkowski, 1964). This two-dimensional pattern can be analysed directly by two-dimensional methods. For example, examination of intact eyes, whole mount preparations and reconstructions of histological sections has enabled the patches of pigmented and albino cells to be visualised in the RPE of chimaeric adult eyes (Mintz, 1971; West, 1976a, 1999; Sanyal & Zeilmaker, 1977; Schmidt et al. 1986; Bodenstein & Sidman, 1987b). This revealed small, randomly orientated patches in the proximal RPE (nearest the optic nerve head) but larger patches, arranged as radial stripes, in the distal RPE (towards the iris). Also, analysis of the distribution of pigmented and albino cells in two-dimensional reconstructions of serial sections of RPE from chimaeras suggested individual patches were often clustered in radial sectors (Sanyal & Zeilmaker, 1977). These radial clusters may represent descendent clones that are fragmented into smaller coherent clones proximally but less fragmented distally (West, 1978), where cell mixing is more limited during the later stages of growth (Bodenstein & Sidman, 1987a,b).

The two-dimensional pattern of patches in the RPE can also be reduced to a set of one-dimensional strings of cells by cutting histological sections. Patches in a one-dimensional string may vary in length and distribution. In a series of pigmented↔albino chimaeric eyes, the likelihood that a single patch of pigmented cells will encompass more than one coherent clone is greater for eyes with higher proportions of pigmented cells. This masks the sizes of the coherent clones and makes it difficult to combine results from chimaeras that have different percentages of black cells.

Two summary statistics have been used to estimate the underlying coherent clone size in histological sections of variegated RPEs from fetal mouse chimaeras (West et al. 1997). One approach was to use a correction factor to allow for the effects of differences in proportion (p) of pigmented cells on the mean patch length. The observed mean patch length was divided by the function $1/(1-p)$, derived by Roach (1968), to convert it to a 'corrected mean patch length'. This approach has been used to evaluate the extent of cell mixing in different tissues (West, 1975, 1976a,b; Mullen, 1977; Oster-Granite & Gearhart, 1981). More recently it has been adapted to compare limbal stem function in different groups of mice during the maintenance of the corneal epithelium (Collinson et al. 2002, 2004; Mort, 2009; Mort et al. 2009). However, it has been shown that coherent clones in the RPE vary in size and that the sizes may not be normally distributed (Schmidt et al. 1986), so while the corrected mean patch length is useful for comparing coherent clone sizes and numbers in different groups of chimaeras it may not provide an accurate estimate of the true mean coherent clone length. The 'corrected mean patch length' is an estimate of the expected mean length of coherent clones that would produce the observed (uncorrected) mean patch length if the coherent clones are randomly distributed and their lengths are either equal or normally distributed.

The second approach was to restrict the analysis to the minority cell population in eyes where the contributions of the two genotypes were grossly unbalanced. In chimaeric eyes where albino cells predominate, most patches of pigmented cells are likely to comprise individual coherent clones and the median patch length of the minority cell population can be used to summarise coherent clone size. Schmidt et al. (1986) analysed the RPEs from four unbalanced chimaeras which all had < 10% pigmented cells in the RPE. One disadvantage of this approach is that it may not be applicable to more balanced chimaeras.

Comparisons of these two summary statistics gave almost identical numerical estimates of coherent clone sizes for the RPE of fetal chimaeras, so validating the use of the corrected mean patch length for the fetal RPE regardless of the percentage of pigmented cells in the RPE (West et al. 1997). However, at this stage there is extensive cell mixing in the RPE and the two methods have yet to be compared in tissues with larger coherent clones, such as the adult RPE.

One-dimensional spatial analysis can also be used to identify two-dimensional striped patterns by comparing the variability in composition of multiple one-dimensional samples collected along each of two or more different orientations. This approach was used to identify radial stripes in chimaeric ovarian follicles (Boland & Gosden, 1994). The proportion of one cell population was estimated along five randomly chosen radial lines (from the oocyte to the periphery of the follicle) and along five concentric rings drawn at intervals outwards from the oocyte. The radial values of p were more variable than the circumferential values, implying that there were alternating stripes of transgenic and wild-type cells radiating from the oocyte to the margin of the follicle.

In the present study we used computer simulations to predict the utility of one-dimensional analysis for discriminating between different two-dimensional distributions of patches and we tested these predictions on variegated patterns in the RPE in histological sections of eyes from fetal and adult mouse chimaeras. This showed that the median patch length for the minority cell population and the corrected mean patch length produced similar estimates of the coherent clone size, which distinguished between different simulated arrays of clumps of cells. Both of these summary statistics also identified differences in distributions of pigmented and albino cells in the RPE of fetal and adult chimaeras. Secondly, we showed that differences in the variance of the percentage of black cells between two series of appropriately orientated, perpendicular transect lines or histological sections could identify the presence of striped distributions of black and white cells in simulated striped arrays and the RPE of adult chimaeras.

Materials and methods

Computer simulations

To simulate a one-dimensional analysis, from tissue sections of two-dimensional chimaeric or mosaic tissues, data were

collected from each row and column of 100×100 arrays. This represents one-dimensional transect lines superimposed on computer simulations of two-dimensional mosaic arrays of black and white squares (representing cells). Data were collected separately from all 100 rows (horizontal transect lines) for each array and summary statistics (mean, standard deviation, etc.) were calculated for each array. Equivalent data were collected and summarised for all 100 columns (vertical transect lines). Data from horizontal and vertical one-dimensional analyses were compared to investigate whether various types of striped distributions of black and white cells could be identified. Means were calculated for the 10 replicate arrays in each of the array sets separately for the horizontal and vertical one-dimensional analyses. The primary data collected for each transect line were % black cells, mean patch length (cells per patch), median patch length and corrected mean patch length of black patches. The corrected mean patch length for black patches is the observed mean patch length of black patches divided by the function $1/(1-p)$, where p is the proportion of black cells in the sample (transect line) as derived by Roach (1968) and discussed elsewhere (West, 1976a; Mort et al. 2009). Equivalent data were collected for the white cells and white patches.

Computer simulations were written in JAVA. For a random distribution, a random number between 0 and 1 was assigned to each of the elements composing the array. To change the pigmentation percentage, a threshold was applied to these values determining if they would be pigmented or non-pigmented. For example, to obtain an average pigmentation of 50%, the threshold was fixed at 0.5, so that if the value is < 0.5 the pixel is pigmented and if it is ≥ 0.5, the pixel is not pigmented. To model patches, the same process was applied by assigning a random number to every second element (horizontally and vertically) for 2×2 patches or to every fourth element (horizontally and vertically) for 4×4 patches. A threshold was applied, as described previously, and the neighbouring pixels forming a square (2×2 or 4×4), with the valued element corresponding to the top left part of it, were given the same value. To model a striped distribution, the threshold determining the pigmentation state of the elements was defined as a sine function dependent on *x* and *y*, allowing us to vary the average pigmentation, the number of stripes and the angle of the stripes. For curved stripe distributions, a random number was only assigned to elements included in an area corresponding to the curved stripe's position and a threshold was applied to establish their pigmentation. All other elements not included in the striped regions were left blank. Unlike the straight light stripes, the curved light stripes were entirely white.

Production of chimaeras

The albino↔pigmented fetal chimaeras in series XM and XP (West & Flockhart, 1994) were, respectively, albino 'AF_2'↔pigmented (C57BL/Ola × CBA/Ca)F_2 and albino 'AF_1' × BALB/c↔pigmented (C57BL/Ola × CBA/Ca)F_2. 'AF_1' is a cross between the albino congenic strain C57BL/Ola.AKR-*Gpi1-s*^{a},*c*/Ws and the albino inbred BALB/c strain. 'AF_2' embryos for chimaera production were produced by intercrosses between two AF_1 mice. E12.5 fetal chimaeras in series CA and adult chimaeras in series AdCA were both albino (BALB/c × A/J)F_2↔pigmented ['TGB' × (C57BL/Ola × CBA/Ca)]F_2. 'TGB' is a transgenic strain, predominantly of (C57BL/Ola × CBA/Ca)F_1 genetic background, that is homozygous (*Tg*/*Tg*) for the β-globin transgene TgN(Hbb-b1)83Clo (Lo, 1986). The transgene was included in these chimaeras for analysis of other tissues (to be reported elsewhere). Chimaeras of three genotype combinations, with respect to the transgene, were included among the albino↔pigmented CA and AdCA chimaeras: −/−↔*Tg*/*Tg* (AdCA20, 21 and 29), −/−↔*Tg*/− (CA5, 9 and 15; AdCA17, 18, 19, 23, 24 and 30) and −/−↔−/− (CA3 and 7). Founder CBA/Ca animals were obtained from the Institute of Cell, Animal and Population Biology, University of Edinburgh. BALB/c and some BF1 mice were purchased from the Department of Medical Microbiology, University of Edinburgh. All other animals were bred and maintained under conventional conditions in the Centre for Reproductive Biology, Edinburgh. Animal work was performed in accordance with institutional guidelines and UK Home Office regulations.

Chimaeras were produced by aggregation of eight-cell stage embryos by conventional methods as previously described (Tarkowski, 1961; Mintz et al. 1973; West & Flockhart, 1994). For analysis of fetal chimaeras, pregnant females were killed at E12.5 days' gestation and the conceptuses were dissected as described elsewhere (West & Flockhart, 1994).

Histological analysis of chimaeric eyes

Heads of fetal chimaeras were fixed in 75% ethanol, 25% acetic acid, processed to paraffin wax in the conventional way, sectioned at 7 μm and stained with haematoxylin and eosin. In some cases part of the fetal head containing one eye was sectioned parasagittally and then the sample was re-embedded and the second eye was sectioned perpendicularly to the first. Patches of pigmented and albino cells in the RPE were measured in single parasagittal sections near the middle of the eye and in equally spaced sections either side of the mid-section. Measurements were made with the COLOUR VISION image analysis software (Improvision, Coventry, UK) running on an Apple Macintosh computer, linked to an Olympus BH2 microscope. The mean patch length, proportion of pigmented cells and estimated cell length were estimated as described previously (West, 1976a; West et al. 1997).

Adult chimaeric eyes were fixed in 75% ethanol, 25% acetic acid overnight, stored in 70% alcohol until photographed and then processed to produce 3-μm plastic sections. Adult eyes were refixed in super fix (164 mM cacodylate, 1 mM picric acid, 3% glutaraldehyde, 2% paraformaldehyde) at 4 °C for 12–14 h. After 2 h in super fix most of the cornea was removed with scissors, under a dissecting microscope, to allow better penetration. The eyes were then washed in 0.05 M maleate buffer pH 5.15 (2×1 h changes), dehydrated through a graded ethanol series and embedded in epon-araldite (Kerr & Sharpe, 1985) with pupils facing either vertically or horizontally. Sections of 3 μm were cut with a Reichart-Jung Supercut 2050 microtome, mounted on glass microscope slides and stained in a 1% solution of toluidine blue (in 1% aqueous borax) for 1 min, rinsed in water and then 70% ethanol. Left and right eyes were sectioned in different planes so the sections would intersect any radial stripes at different angles and patches of pigmented or albino cells were measured as described for the fetal eyes. If the eye is orientated so the proximal-distal axis is vertical, left eyes were sectioned in the horizontal ('latitudinal') plane and right eyes in the vertical ('longitudinal plane').

Two-dimensional reconstructions of pigmented patches in RPEs of fetal chimaeras

Planar and annular, two-dimensional reconstructions of pigmented patches in the RPE were produced from measurements of one-dimensional lengths of pigmented and albino stretches of RPE in serial sections of regions of chimaeric fetal eyes. Planar reconstructions of the length of pigmented and albino eyes, stretches of the RPE in adjacent sections were made using a series of horizontal stacked bar charts. The total length of each horizontal bar represented the circumference of a single section of the eye and the bar was divided into black and white sections according to the lengths of the pigmented and albino patches. A two-dimensional reconstruction was built by stacking a series of horizontal bars, representing adjacent sections, on top of each other in the correct order and aligning their midpoints. This produced a symmetrical arrangement of bars (representing histological sections) of different lengths. The horizontal and vertical scales were adjusted to maintain the correct aspect ratio.

Annular reconstructions of pigmented patches were produced from uniform-sized black and white pie charts, one for each section of the eye, using the patch length data. The pie charts were re-sized and stacked and the size of the pie chart for the longest circumference (middle section) was designated 100%. Pie charts for successive adjacent sections in one direction were reduced in size by 1% per chart and pie charts for adjacent sections on the other side of the longest section were increased in size by 1% per chart. The pie charts were then aligned about their centres and stacked on top of each another with the largest at the bottom. A white disk that was 1% smaller than the smallest pie chart was placed on top of the stack.

Statistics

Statistical tests were performed on an Apple Macintosh computer using GRAPHPAD PRISM, STATVIEW and Microsoft EXCEL software.

Results

One-dimensional analysis of computer simulations of two-dimensional patches and stripes

Computer simulations of black and white mosaic tissues comprising 100×100 arrays of cells were produced as described in the Materials and methods section. Eleven different types of arrays were compared. The first four were: (i) random distribution of black and white cells, (ii) random distribution of 2×2 clumps of four cells, (iii) random distribution of 4×4 clumps of 16 cells and (iv) curved striped array comprising curved dark and light stripes, where the dark stripes contain both black and white cells and the light stripes contain only white cells. A further seven types of striped arrays (array types 5–11) with straight dark and light stripes (comprising predominantly black and white cells, respectively) orientated at different angles from the vertical were also analysed: (5) 0° (vertical) stripes, (6) 12° stripes, (7) 30° stripes, (8) 45° stripes, (9) 60° stripes, (10) 78° stripes and (11) 90° (horizontal) stripes. For each of these 11 array types, nine sets of 10 replicate arrays were simulated. The nine array sets differed in the total percentage of black cells in the array. For most types of arrays the array sets varied from 10 to 90% black cells in 10% steps (or approximately 10% steps for the straight stripes) but for the curved stripes the nine sets varied from 10 to 60% black cells. A total of 990 different 100×100 cell, two-dimensional arrays were simulated and analysed (11 array types $\times$ 9 array sets $\times$ 10 replicates). Each two-dimensional array represents a simulation of a square mosaic or chimaeric tissue of 10 000 cells with variable percentages and distributions of black and white cells. The random distributions of cells represent tissues that have undergone extensive cell mixing during development (non-coherent clonal growth) and the clumped arrays represent tissues with different extents of limited coherent clonal growth. The 2×2 and 4×4 clumped arrays represent simulations of tissues with uniform coherent clone sizes of 4 and 16 cells (coherent clone lengths of 2 and 4 cells), respectively. The striped arrays simulated tissues with elongated but fragmented descendent clones.

Variation in mean, median and corrected mean patch lengths in random and clumped arrays

Figure 1 shows the effect of varying the percentage of black cells in the array on the mean, median and corrected mean patch length for black and white patches in nine sets of arrays (10–90% black) for each of four different types (random, 2×2 clumps, 4×4 clumps and curved stripes). This is shown separately for horizontal and vertical patch lengths for both black and white patches. (There are four distributions per figure in E–P but results for vertical and horizontal arrays are very similar and so are superimposed.) Each point plotted represents the mean ± SEM of data from 10 replicates of 100 transect lines. For the randomly orientated distributions (random cells and clumps of cells) the mean length of the black patches appears to increase exponentially as the percentage of black cells increases (Fig. 1E–G). As expected, the distributions for black and white mean patch lengths were inversely related and the mean length of the white patches increased with increasing percentage of white cells (decreasing percentage of black cells), so only the black patches are considered in Figs 2–5. In each case for Fig. 1E–G, a two-way ANOVA showed that uncorrected patch length was significantly affected by the percentage black cells in the array ($P < 0.001$ in each case) but there was no overall affect of transect orientation (horizontal vs. vertical) or interaction between transect orientation and percentage black.

The median patch lengths (Fig. 1I–K) showed flatter distributions with median black patch length increasing when the percentage of black cells was highest and the median white patch length increasing when the percentage of black cells was lowest. For arrays with random distributions of black and white cells (Fig. 1I) the median black patch

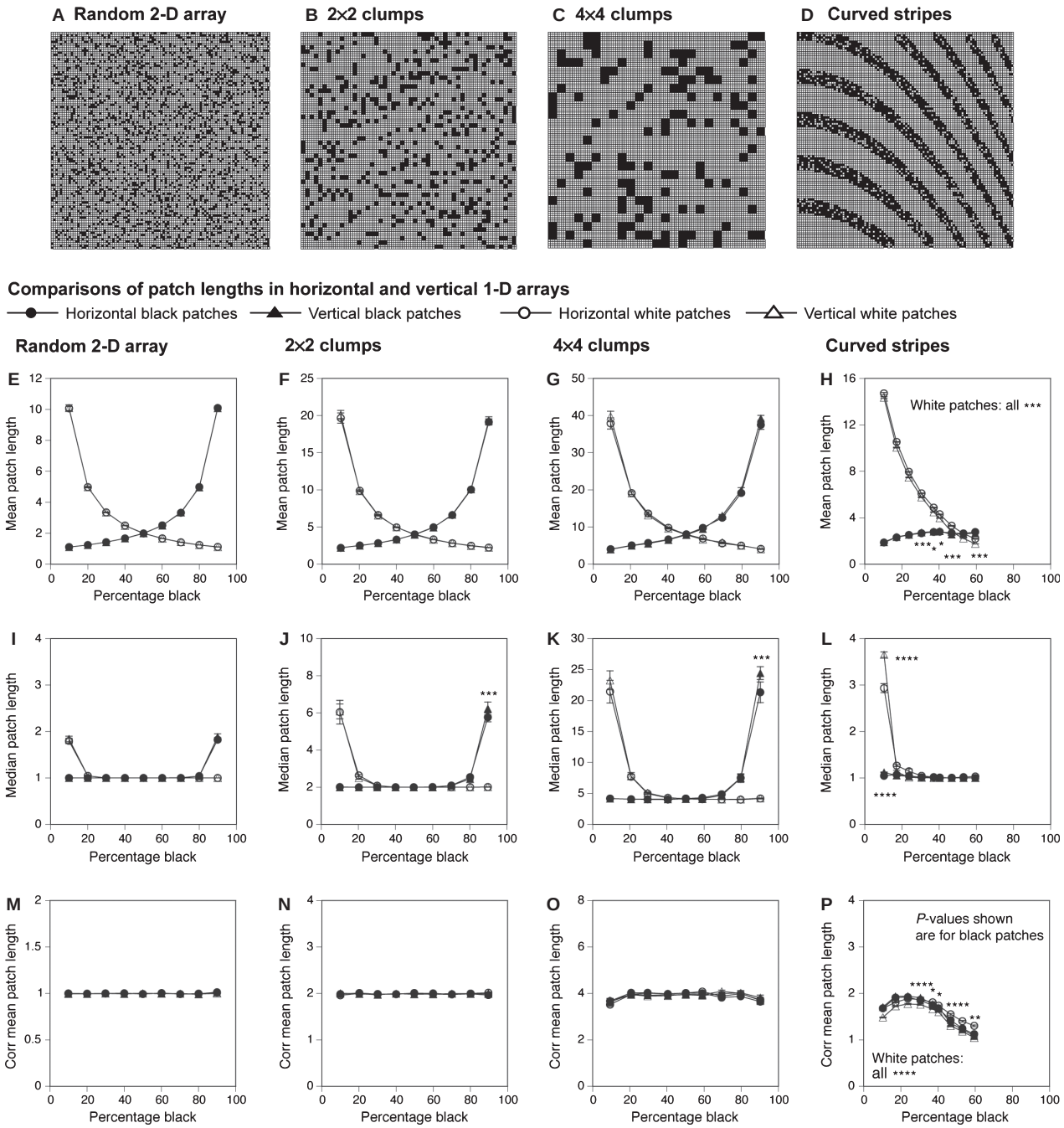

Fig. 1 Patch length analysis using one-dimensional information from two-dimensional computer simulations of random, clumped and curved stripe arrays. (A–D) Illustrations of four types of arrays of 100 × 100 cells: (A) Random distribution of black and white cells. (B) Random distribution of clumps of four cells (2 × 2 clumps). (C) Random distribution of clumps of 16 cells (4 × 4 clumps). (D) Array comprising curved dark and light stripes, where the dark stripes contain both black and white cells and the light stripes contain only white cells. (E–P) Relationships between the percentage black cells in the arrays and (E–H) mean patch length, (I–L) median patch length and (M–P) corrected mean patch length. The horizontal and vertical patch length distributions are plotted separately for black and white patches in E–P (four plots shown per figure but some are superimposed). *P*-values shown by asterisks in the figures are for comparisons of mean, median or corrected mean patch lengths for horizontal vs. vertical transects. Separate comparisons for black and white patches for each set of arrays were made by Bonferroni *post-hoc* tests if a two-way ANOVA with repeated measures showed transect orientation or interaction between transect orientation and percentage black had a significant overall effect on patch length across all array sets. Other statistical comparisons are discussed in the text. (*$P < 0.05$; **$P < 0.01$; ***$P < 0.001$; ****$P < 0.0001$.)

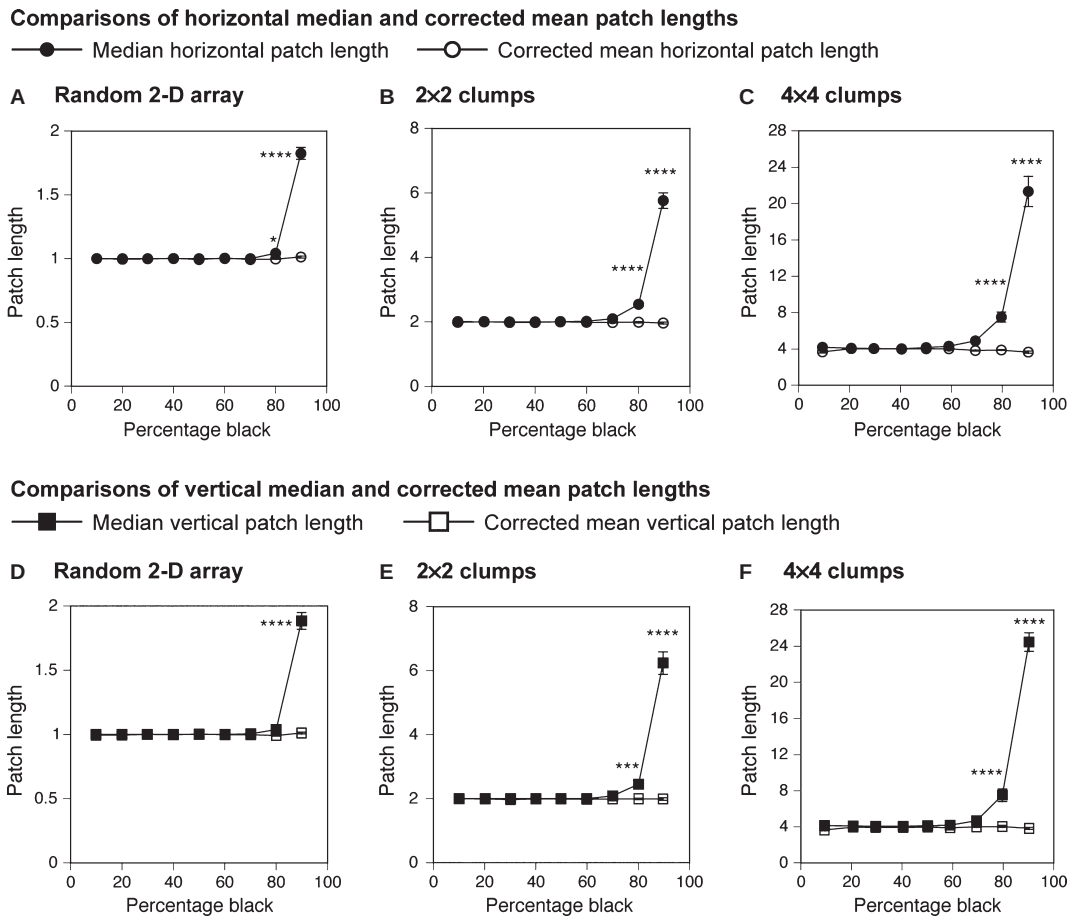

Fig. 2 Comparison of median patch length and corrected mean patch length in simulations of random and clumped arrays. (A–C) Relationships between the median patch length and corrected mean patch lengths in one-dimensional horizontal transect lines from two-dimensional simulations of (A) random arrays, (B) clumps of four cells (2 × 2 clumps) and (C) clumps of 16 cells (4 × 4 clumps). (D–F) Relationships between the median patch length and corrected mean patch length in one-dimensional vertical transect lines from two-dimensional simulations of (D) random arrays, (E) clumps of four cells (2 × 2 clumps) and (F) clumps of 16 cells (4 × 4 clumps). In each case a two-way ANOVA with repeated measures showed that, overall, the patch length was affected by the type of summary statistic (median or corrected mean), the percentage black cells and the interaction between them. *P*-values shown in the figure are for Bonferroni *post-hoc* tests comparing median patch length vs. corrected mean patch lengths separately for each array set. (*$P < 0.05$; **$P < 0.01$; ***$P < 0.001$; ****$P < 0.0001$.)

length was 1.0 cell for most arrays with 10% black cells but increased in arrays with at least 80% black cells. Similar trends were seen for horizontal and vertical transect lines and for black and white patches with the increase in median white patch length occurring below 20% black cells (above 80% white cells). The median black patch length was more sensitive to the percentage of black cells in arrays with 2 × 2 clumps or 4 × 4 clumps of cells (Fig. 1J,K) than in the random arrays (Fig. 1I) but the median length of black patches was close to the predicted values if only 10–50% black arrays were considered (Table 1). One-way ANOVA confirmed that the percentage of black cells in the array had less effect if only arrays with 10–50% black cells were included or if all the array sets were included but the median patch length of the minority cell population (i.e. black cells for arrays with ≤ 50% black cells and white cells for arrays with > 50% black cells) was used (Table 1). Thus, the median patch length of the minority cell population (≤ 50%) correctly identified the clump length (simulated coherent clone length) in the three array types as approximately 1, 2 and 4 cells, respectively (Table 1).

The corrected mean black patch lengths (Fig. 1M–O) were less affected by high percentages of black cells than the medians and the same trend was seen for the results for the white patches. Overall, the corrected mean patch lengths were close to the expected values of 1, 2 and 4 cells, respectively, for the three array types for all the array sets studied, as shown by the mean values (and ranges) for the corrected mean horizontal and vertical patch lengths of random, 2 × 2 and 4 × 4 arrays (Table 1).

The median and corrected mean patch lengths were compared directly in horizontal and vertical transects from random arrays and the two types of clumped arrays by two-way ANOVA with repeated measures. In each case the patch

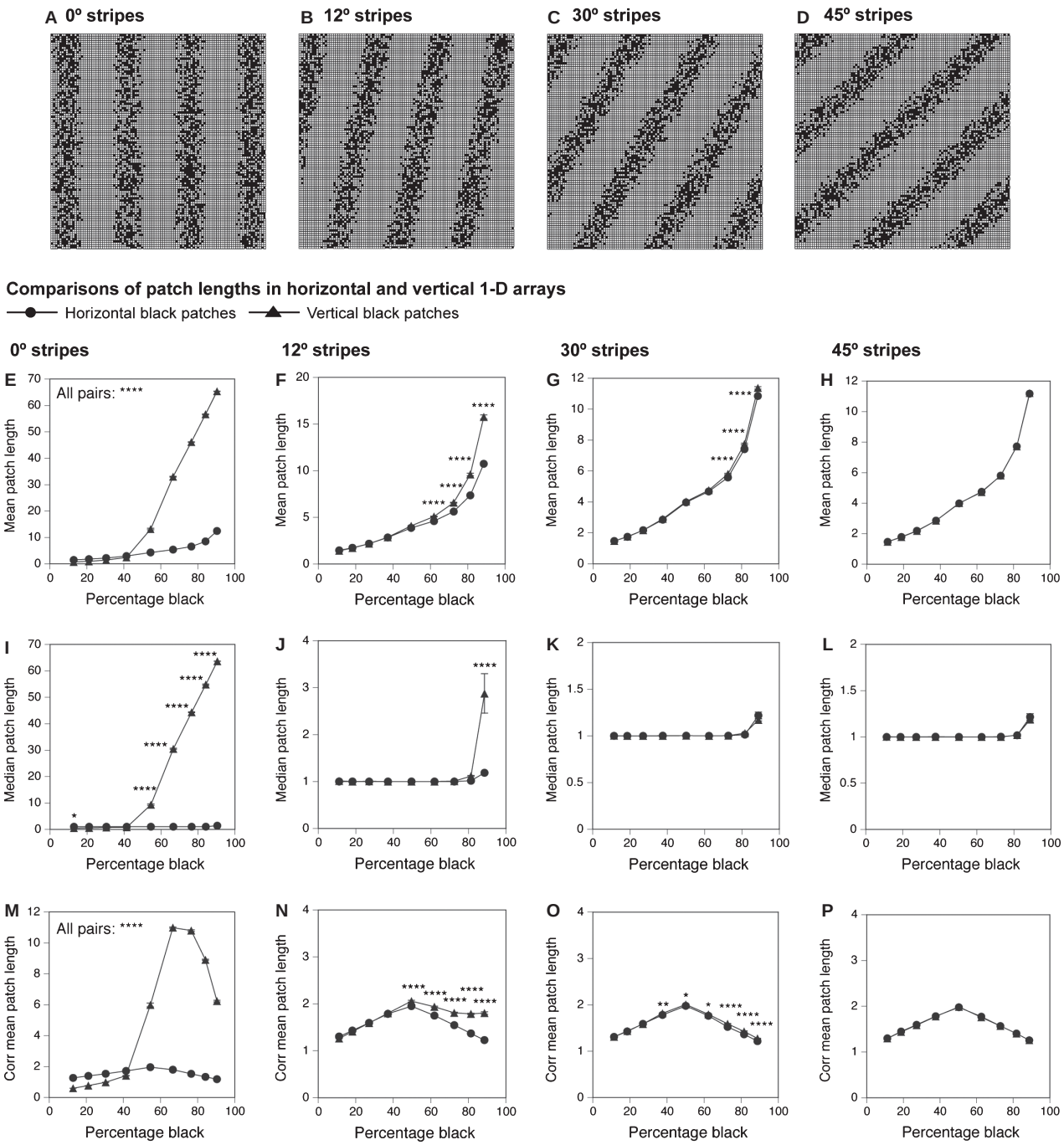

Fig. 3 Patch length analysis using one-dimensional information from two-dimensional computer simulations of striped arrays. (A–D) Illustrations of four types of striped 100 × 100 arrays, comprising straight dark and light stripes, where the dark stripes contain predominantly black cells and the light stripes predominantly white cells. (A) Vertical stripes (0° from the vertical). (B) Stripes orientated 12° from the vertical. (C) Stripes orientated 30° from the vertical. (D) Stripes orientated 45° from the vertical. (E–P) Relationships between the percentage black cells in the arrays and (E–H) mean patch length, (I–L) median patch length and (M–P) corrected mean patch length. *P*-values shown in the figure are for comparisons of results from horizontal vs. vertical transects that were made for each set of arrays by Bonferroni *post-hoc* tests if a two-way ANOVA with repeated measures showed transect orientation or interaction between transect orientation and percentage black had a significant overall effect on patch length. (*$P < 0.05$; **$P < 0.01$; ***$P < 0.001$; ****$P < 0.0001$.) 'All Pairs: ****' (in E and M) means that pairwise *post-hoc* tests comparing patch lengths in horizontal vs. vertical transects were highly statistically significant with $P < 0.0001$ for all nine array sets.

length was affected by the type of summary statistic (median or corrected mean), the percentage black cells and the interaction between them. Bonferroni *post-hoc* tests showed that statistically significant differences between the median and corrected mean patch lengths were confined to arrays with 80–90% black cells and so confirmed that the

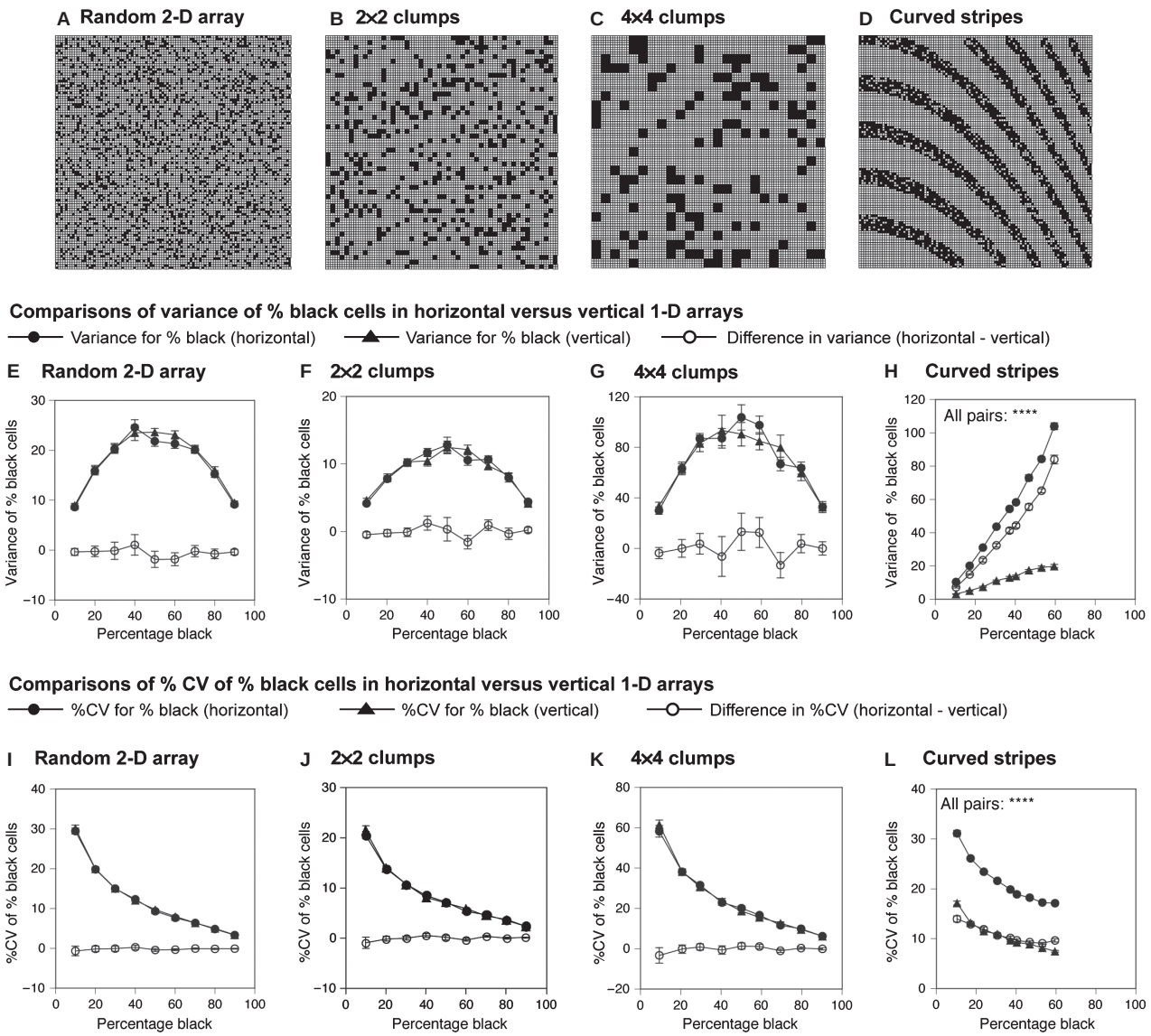

Fig. 4 Variation in percentage black cells in one-dimensional transects of two-dimensional computer simulations of random, clumped and curved stripe arrays. (A–D) Illustrations of four types of arrays of 100 × 100 cells as described in Fig. 1. (E–H) Relationships between the total percentage black cells in the arrays and the variance of the percentage black cells, shown separately for the horizontal transects and the vertical transects. The difference between variances for horizontal and vertical transects (h–v) is also shown. (I–L) Relationships between the total percentage black cells in the arrays and the percentage coefficient of variation (%CV) of the percentage black cells shown separately for the horizontal transects and the vertical transects. The difference between the %CV for horizontal and vertical transects (h–v) is also shown. *P*-values shown in the figure are for comparisons of results from horizontal vs. vertical transects that were made for each set of arrays by Bonferroni *post-hoc* tests if a two-way ANOVA with repeated measures showed transect orientation or interaction between transect orientation and percentage black had a significant overall effect on the variance or the percentage coefficient of variation of the percentage black cells. 'All Pairs: ****' means that pairwise *post-hoc* tests comparing variance (in H) or %CV (in L) in horizontal vs. vertical transects were highly statistically significant with $P < 0.0001$ for all nine array sets. No pairwise comparisons in E–G or I–K were significant.

median and corrected mean were numerically very similar for arrays with up to 50% black cells (Fig. 2). Thus, the median patch length of the minority cell population and the corrected mean patch length were both able to distinguish between random and clumped arrays. Neither the horizontal nor vertical corrected mean black patch lengths were significantly correlated with the percentage of black cells, which shows that the correction factor was effective (Table 2). In contrast, the median pigmented patch lengths were strongly positively correlated with the percentage of black cells. Although in some cases the median patch length of the minority cell population was also correlated with the percentage of minority cell population, the correlation was negative and the range of median patch lengths was

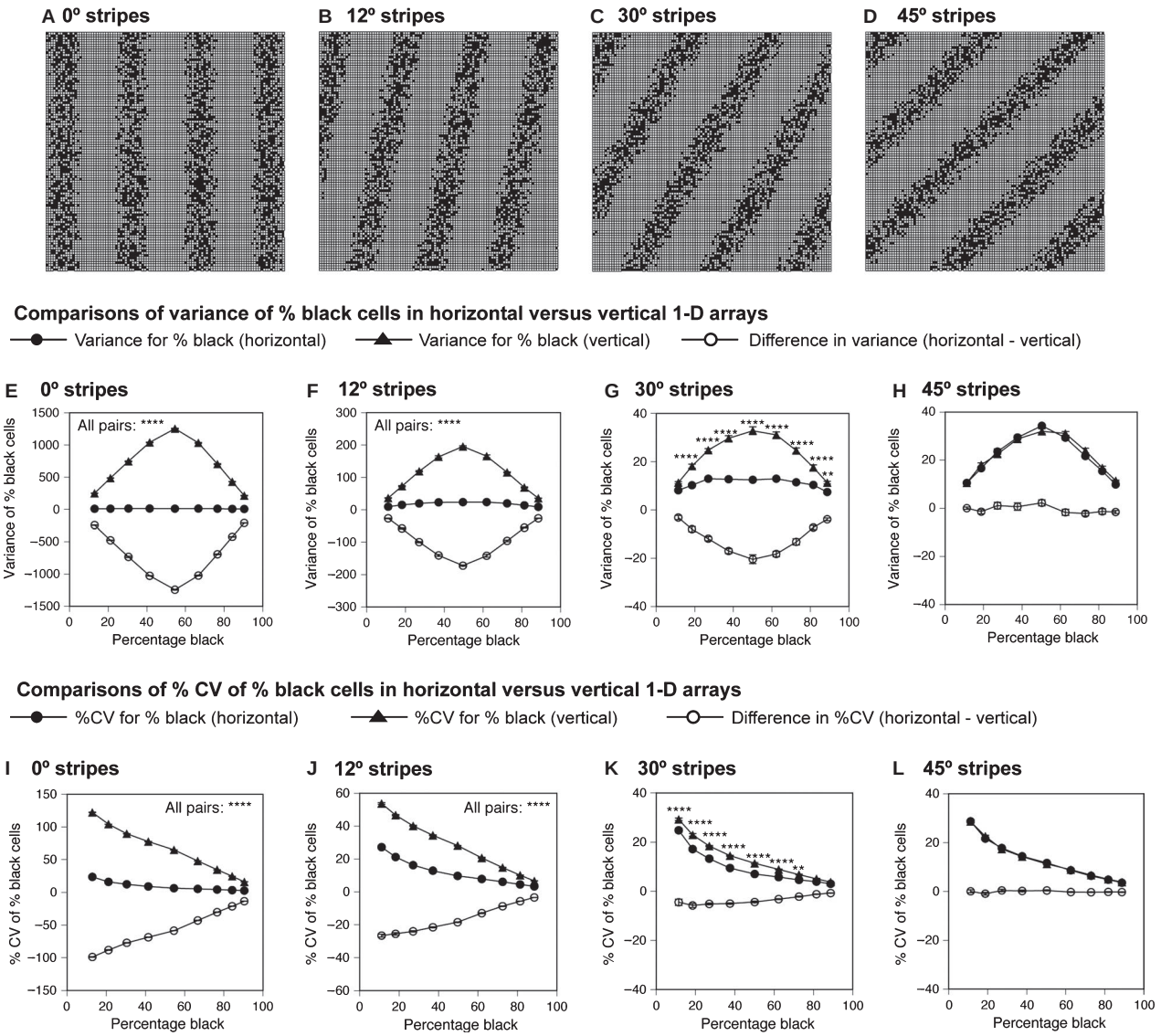

Fig. 5 Variation in percentage black cells in one-dimensional transects of two-dimensional computer simulations of striped arrays. (A–D) Illustrations of four types of striped 100 × 100 arrays, as described in Fig 3. (E–H) Relationships between the total percentage black cells in the arrays and the variance of the percentage black cells, shown separately for the horizontal transects and the vertical transects. The difference between variances for horizontal and vertical transects (h–v) is also shown. (I–L) Relationships between the total percentage black cells in the arrays and the percentage coefficient of variation (%CV) of the percentage black cells shown separately for the horizontal transects and the vertical transects. The difference between the %CV for horizontal and vertical transects (h–v) is also shown. *P*-values shown in the figure are for comparisons of results from horizontal vs. vertical transects that were made for each set of arrays by Bonferroni *post-hoc* tests if a two-way ANOVA with repeated measures showed transect orientation or interaction between transect orientation and percentage black had a significant overall effect on the variance or the percentage coefficient of variation of the percentage black cells. (**P* < 0.05; ***P* < 0.01; ****P* < 0.001; *****P* < 0.0001.) 'All Pairs: ****' means that pairwise *post-hoc* tests comparing variance (in E and F) or %CV (in I and J) in horizontal vs. vertical transects were highly statistically significant with *P* < 0.0001 for all nine array sets.

narrow. These observations imply that the median patch length of the minority cell population accurately identified the clump size in the random and clumped arrays. This was true not just for unbalanced arrays, equivalent to the unbalanced chimaeric tissues considered in previous studies (Schmidt et al. 1986; West et al. 1997), but also for balanced arrays, at least for the relatively small clump sizes simulated in this study.

Variation in mean, median and corrected mean patch lengths in striped arrays

Various arrays of dark and light stripes were analysed. The straight dark stripes contained mostly black cells and the straight light stripes mostly white cells. Although the curved dark stripes contained both black and white cells, the curved light stripes contained only white cells. No

Table 1 Effects of varying the percentage black cells in the array on the median and corrected mean length of horizontal and vertical black patches.

Comparison	Random (1 × 1) arrays	2 × 2 arrays	4 × 4 arrays
Mean and range of black patch length summary statistics for all 90 arrays (10–90% black)			
Median (horizontal)	1.10 (1.00–2.02)	2.49 (2.00–6.52)	6.50 (4.00–30.40)
Median (vertical)	1.10 (1.00–2.36)	2.53 (2.00–8.20)	6.81 (3.68–29.92)
Corrected mean (horizontal)	1.00 (0.98–1.03)	1.99 (1.79–2.11)	3.90 (2.94–4.43)
Corrected mean (vertical)	1.00 (0.98–1.04)	1.99 (1.88–2.20)	3.90 (3.20–4.86)
Mean and range of black patch length summary statistics for 50 arrays with 10–50% black cells			
Median (horizontal)	1.00 (1.00–1.01)	2.00 (2.00–2.04)	4.10 (4.00–4.64)
Median (vertical)	1.00 (1.00–1.00)	2.00 (2.00–2.04)	4.10 (3.68–4.32)
Corrected mean (horizontal)	1.00 (0.98–1.02)	2.00 (1.92–2.11)	3.95 (2.94–4.43)
Corrected mean (vertical)	1.00 (0.98–1.02)	1.99 (1.92–2.09)	3.88 (3.29–4.28)
Mean and range of patch length summary statistics for the minority cell population in 90 arrays			
Median (horizontal)	1.00 (1.00–1.01)	2.00 (2.00–2.08)	4.08 (4.00–4.80)
Median (vertical)	1.00 (1.00–1.00)	2.00 (2.00–2.04)	4.10 (3.68–4.48)
Differences among array sets (different % black): *P*-values from 1-way ANOVA (10–90% black arrays)			
Median (horizontal)	$P < 0.0001$	$P < 0.0001$	$P < 0.0001$
Median (vertical)	$P < 0.0001$	$P < 0.0001$	$P < 0.0001$
Corrected mean (horizontal)	$P = 0.0063$	NS	$P = 0.0004$
Corrected mean (vertical)	$P = 0.0169$	NS	$P = 0.0099$
Differences among array sets (different % black): *P*-values from one-way ANOVA (10–50% black arrays)			
Median (horizontal)	NS	$P = 0.0089$	NS
Median (vertical)	NS	NS	NS
Corrected mean (horizontal)	NS	NS	$P = 0.0038$
Corrected mean (vertical)	NS	NS	$P = 0.0012$
Differences among array sets: *P*-values from one-way ANOVA (minority cell population in 10–90% arrays)			
Median (horizontal)	NS	NS	$P < 0.0131$
Median (vertical)	NS	$P < 0.0112$	$P < 0.0318$

NS, not statistically significant.

Table 2 Kendall correlations between different summary statistics of patch lengths and the percentage composition of three types of simulated arrays.

Comparison	Random (1 × 1) arrays	2 × 2 arrays	4 × 4 arrays
Correlations with black patch lengths			
Median (horizontal) vs. % black	0.557; $P < 0.0001$	0.661; $P < 0.0001$	0.624; $P < 0.0001$
Median (vertical) vs. % black	0.651; $P < 0.0001$	0.664; $P < 0.0001$	0.564; $P < 0.0001$
Corrected mean (horizontal) vs. % black	0.016; $P = 0.82$ (NS)	−0.043; $P = 0.55$ (NS)	−0.095; $P = 0.19$ (NS)
Corrected mean (vertical) vs. % black	0.050; $P = 0.48$ (NS)	−0.059; $P = 0.41$ (NS)	0.097; $P = 0.18$ (NS)
Correlations with median patch lengths of minority cell population			
Median (minor; horizontal) vs. % minor	−0.119; $P = 0.097$ (NS)	−0.222; $P = 0.0020$	−0.082; $P = 0.25$ (NS)
Median (minor; vertical) vs. % minor	−0.127; $P = 0.075$ (NS)	−0.214; $P = 0.0029$	−0.177; $P = 0.0135$

Kendall rank-correlation coefficients corrected for ties (τ) are shown with *P*-values.
NS, not statistically significant.

clumps of cells were deliberately included in the stripes and they were intended to simulate discontinuous descendent clones rather than coherent clones. The curved striped arrays (Fig. 1H,L,P) were analysed for 10–60% black cells and showed similar trends for mean patch length and median patch length to the random and clumped arrays over the same range. However, the corrected mean patch length was more affected by variation in the percentage of black cells in the curved striped arrays than in the random and clumped arrays. The curved stripes also showed more differences between results for horizontal and vertical transect lines. These would intersect curved stripes at different angles in different places in the array, so to investigate the effects of the angle of intersection a series of arrays with straight stripes was analysed.

Figure 3 shows the effect of varying the percentage of black cells in the array on the mean, median and corrected mean patch lengths for black patches in nine sets of arrays for each of four types of striped arrays in which the stripes were orientated, respectively 0°, 12°, 30° and 45° from the vertical. (Three additional array types were analysed with stripes orientated 60°, 78°, and 90° from the vertical but these are not illustrated as they yielded similar results to the 30°, 12°, and 0° stripes, respectively, except that their relationships to the horizontal and vertical transects were reversed.)

The mean patch length for all four types of stripes shown in Fig. 3A–D increased as the percentage of black cells in the array increased (Fig. 3E–H). For vertical (0°) striped arrays the mean patch lengths were significantly greater in the vertical transect lines than the horizontal patch lengths and this difference narrowed progressively for 12°, 30° and 45° striped arrays. The difference in mean horizontal and vertical black patch lengths seen in arrays with vertical or near-vertical stripes presumably reflects the limit imposed on the maximum length of horizontal black patches by the light stripes. In 45° striped arrays there was no difference between horizontal and vertical mean patch lengths (Fig. 3H) and the effect of variation in the percentage of black cells on the mean black patch length appeared similar to its effect in the random arrays (Fig. 1E).

The median patch length followed a similar trend to the mean patch length with significant differences between horizontal and vertical median patch lengths in vertical striped arrays and the 12° striped arrays with the highest percentage of black cells but not in 30° or 45° striped arrays. Again, the effect of variation in the percentage black cells on the median black patch length in the 45° striped arrays (Fig. 3L) appeared similar to the random arrays (Fig. 1I). The median patch lengths in the 45° striped arrays were close to one cell for most array sets.

The horizontal and vertical corrected mean patch lengths also differed in all the vertical striped arrays (Fig. 3M) and in some of the 12° and 30° striped arrays (with higher percentages of black cells; Fig. 3N,O) but not in 45° striped arrays (Fig. 3P). However, the effect of variation in the percentage black cells on the corrected mean black patch length in the 45° striped arrays (Fig. 3P) was not the same as in the random arrays (Fig. 1M). In the random arrays the corrected mean patch length was approximately 1 cell for arrays with 10–90% black cells but in the 45° striped arrays it rose from 1.3 cells in arrays with 10% black cells to a maximum of 2.0 with 50% black cells and then declined back to 1.3 with 90% black cells. The corrected mean horizontal patch lengths in the vertical, 12° and 30° striped arrays also showed a peak value at 50% black cells.

For arrays with 50% black cells ($P = 0.5$), dividing a mean black patch length of 4.0 by the correction factor $1/(1-p)$ equates to dividing it by 2 to give a corrected mean black patch length of 2.0. However, most of the black cells are in dark stripes and the size of most black patches will be affected by the percentage of black cells in the immediate neighbourhood (i.e. the dark stripes) rather than the array as a whole. If the typical percentage of black cells in the dark stripes was closer to 75% ($P = 0.75$) it would be more appropriate to divide the observed mean patch length by $1/(1-0.75)$ than $1/(1-0.5)$. This would halve the value of the corrected mean patch length for 45° striped arrays with 50% black cells (Fig. 3P) to 1.0 and make it similar to the median patch length for the 45° striped arrays (Fig. 3I). Thus, the failure of the corrected mean patch length to compensate evenly for the effects of the percentage of black cells appears to be a consequence of the uneven distribution of black and white cells in striped arrays, which results in under-correction of the mean patch length. Inappropriate correction factors probably also explain the unusual shapes of the graphs for the corrected mean patch length for the curved stripes (Fig. 1D) and the corrected mean vertical black patch lengths for the straight vertical stripes (Fig. 3M). Thus, although the median patch length of the minority cell population and the corrected mean patch length were both able to distinguish between random and clumped arrays, the corrected mean patch length performed less well when black and white cells were arranged as discontinuous stripes.

Distinguishing clumped and striped distributions by one-dimensional analysis of two-dimensional arrays

Black and white cells in mosaic or chimaeric tissues may form stripes either because the underlying coherent clones are elongated in a specific direction or because the coherent clones are non-randomly distributed in the tissue. In either case it is expected that the percentage of black cells in a series of one-dimensional transect lines approximately parallel to the stripes would be more variable than a series of transect lines that are approximately perpendicular to the stripes. To test this, the variance and percentage coefficient of variation (%CV) of the percentage of black cells were compared for two series of perpendicular transects (horizontal and vertical) for randomly orientated arrays (Fig. 4E–G and Fig. 4I–K), curved arrays (Fig. 4H,L) and striped arrays with straight stripes orientated 0°, 12°, 30° and 45° from the vertical (Fig. 5). However, first the mean patch length, median patch length and corrected mean patch length were compared between horizontal and vertical transects of these arrays (Figs 1 and 3). Significant differences between horizontal and vertical transects for various parameters are shown in Figs 1, 3, 4 and 5 and were calculated by Bonferroni *post-hoc* tests if a two-way ANOVA with repeated measures was significant for the parameter under test or its interaction with the percentage black cells.

The mean patch lengths were very similar for the horizontal and vertical transect lines in random and clumped distributions (Fig. 1E–G) and, as already noted, two-way repeated measures ANOVAs showed no significant overall

effect of transect orientation or any interaction between transect orientation and percentage black for either black or white patches in Fig. 1E–G. There were a few significant but small differences between horizontal and vertical median patch lengths (Fig. 1I–K) but none for the corrected mean patch lengths (Fig. 1M–O). As noted above, the curved stripes showed more differences between results for horizontal and vertical transect lines (Fig. 1H,L,P). For the curved arrays, two-way ANOVAs showed that the mean, median and corrected mean patch length were all significantly affected by the transect orientation and/or the interaction between transect orientation and percentage black. Significance levels for Bonferroni *post-hoc* tests are shown in Fig. 1H,L,P; the patch length differences were relatively small. Greater differences between horizontal and vertical mean, median and corrected mean patch lengths occurred for some of the arrays of straight stripes but they were only significant for all percentages of black patches, for the mean and corrected mean patch lengths of the vertical stripes (Fig. 3E,M). This suggests that differences in patch lengths in perpendicular pairs of transect lines can only identify stripes produced by differences in distributions of black and white cells consistently if one of the transect lines is nearly parallel to the stripes.

The variance and %CV were calculated separately for 100 horizontal and 100 vertical transects in each array and the mean ± SEM were plotted for the 10 replicates for each of the nine array sets for each array type. The variance and %CV of the percentage of black cells did not differ in the vertical vs. the horizontal transects in any of the random and clumped arrays (Fig. 4E–G and Fig. 4I–K) but differed for all of the curved arrays (Fig. 4H,L), all of straight stripes orientated 0° or 12° from the vertical (Fig. 5E,F,I,J) and most of the straight stripes orientated 30° from the vertical (Fig. 5G,K). The magnitude of the vertical variances peaked in arrays with 50% of black cells overall (Fig. 5E–H). For vertical 12° and 30° stripes, the differences between the vertical and horizontal variances were also maximal for arrays with 50% black cells (Fig. 5E–G). In arrays of nearly vertical stripes with 50% black cells, approximately 50% of the vertical transects will be mainly in the dark stripes (predominantly black cells) and 50% will be mainly in the light stripes (predominantly white cells), so maximising the variance. In contrast, the maximum %CV values and biggest differences between horizontal and vertical %CV values occurred when the percentage of black cells was low, presumably because the mean percentage of black cells is used as the denominator when calculating the %CV. As expected, there were no significant differences in variance or %CV of the percentage of black cells between the horizontal and vertical transects for the 45° stripes and any differences were small (Fig. 5H,L). Thus, comparison of the variance and %CV of the percentage of black cells in two series of perpendicular transect lines was able to distinguish most striped arrays from random or clumped arrays as long as the two series of transect lines intersected the stripes at different angles (i.e. not both close to 45°).

Two-dimensional patterns of patches in the RPE of mouse chimaeras

The analysis of computer simulations described above made two predictions that are relevant to the analysis of two-dimensional chimaeric and mosaic patterns in one-dimensional sections.

1 The median patch length of the minority cell population and the corrected mean patch length provide similar estimates of the coherent clone length, which should distinguish between chimaeric or mosaic tissues with different extents of cell mixing.

2 Differences in the variance, of the percentage of one of the cell populations in a chimaeric or mosaic tissue, between pairs of perpendicular sections should identify whether descendent clones of cells are arranged as stripes provided that the two types of sections intersect the stripes at sufficiently different angles.

Histological analysis of chimaeric retinal pigment epithelia was undertaken to test these predictions but first the

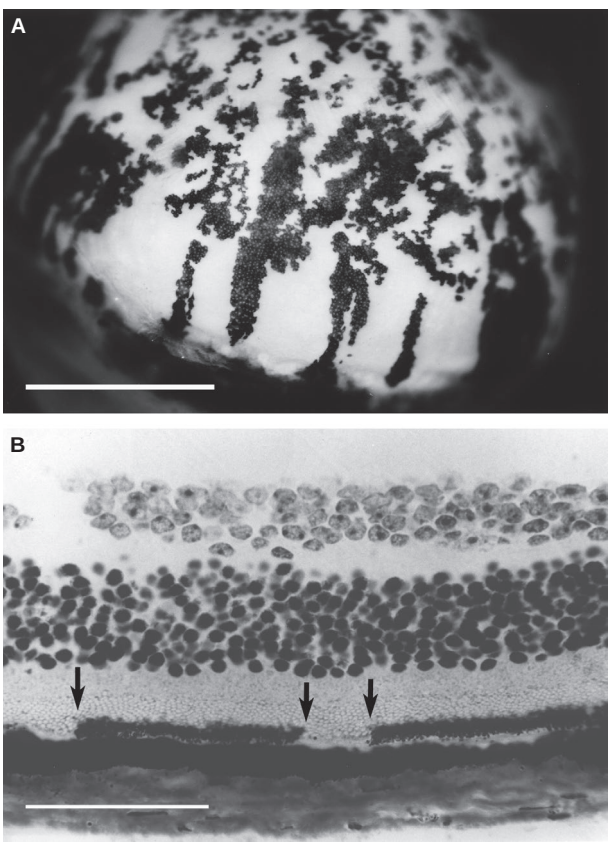

Fig. 6 (A) Side view of the left eye of adult chimaera AdCA18 showing stripes in the RPE towards the iris (bottom of figure). Scale bar: 1 mm. (B). Plastic section of adult eye of chimaera AdCA29 showing patches in RPE (arrows). Scale bar: 50 μm.

two-dimensional patterns of variegation were characterised by two-dimensional methods. In adult, pigmented↔albino chimaeras, the RPE is usually obscured by pigment in the overlying choroid but in some chimaeras the choroid is predominantly unpigmented and this allows the patches in the RPE to be visualised directly in the intact eye. This is

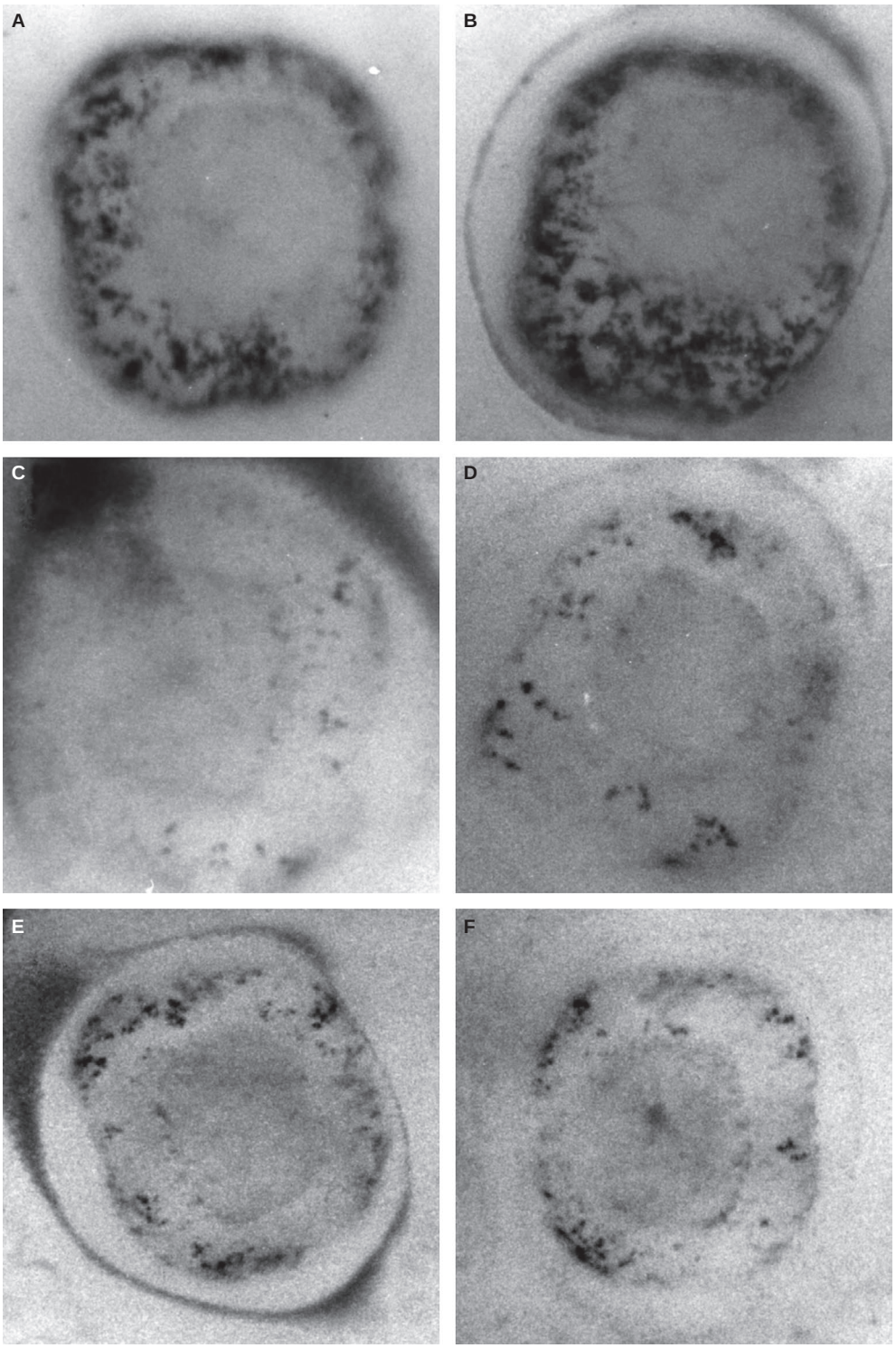

Fig. 7 Intact left (A,C,E) and right (B,D,E) eyes of E12.5-day chimaeras showing patch distribution of pigmented cells in the RPE. (A,B) chimaera XM24; (C,D) chimaera XM28; (E,F) chimaera XP19. (Results of the analysis of mid-sections of eyes from chimaeras XM28 and XP19 are shown in Table 3 and two-dimensional reconstructions of RPE pigment distributions are shown in Fig. 8.) The diameter of each eye is approximately 0.5 mm.

illustrated in Fig. 6A, which confirms previous observations of radial stripes in the distal RPE, towards the iris (see Introduction).

Analysis of the pattern of RPE growth suggests that formation of stripes by edge-biased growth does not begin until the late fetal stage (Bodenstein, 1986; Bodenstein & Sidman, 1987a). Examination of fetal eyes *in situ* with low levels of pigment provides evidence for clumping of pigmented cells but not for clearly defined stripes (Fig. 7). However, the reconstructions of pigmentation patterns in

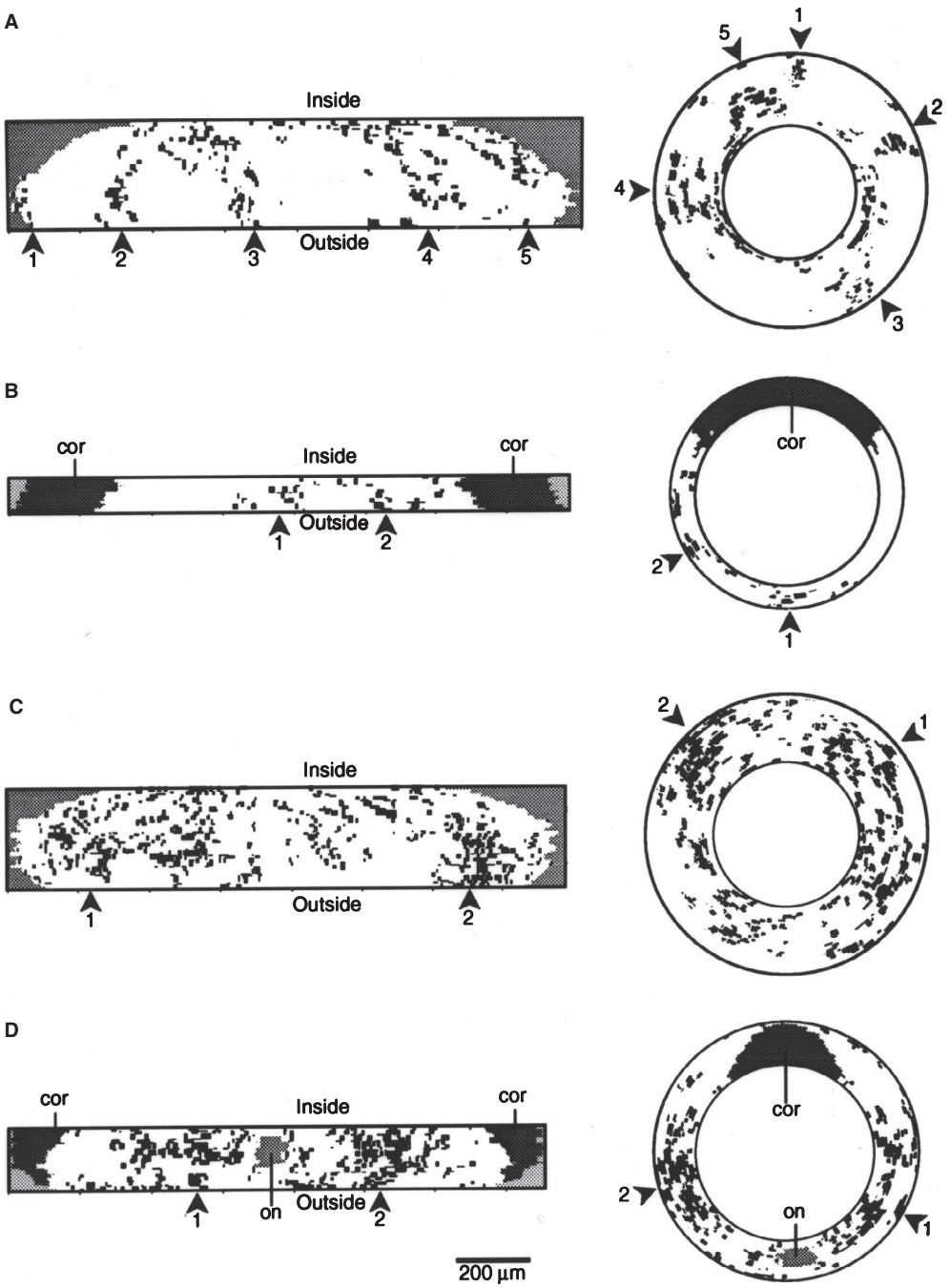

Fig. 8 Diagrams of two-dimensional reconstructions of RPE pigment patterns from one-dimensional measurements of patch lengths in sections of fetal chimaeric eyes. Each pair of diagrams shows a planar (left) and annular (right) reconstruction of the same eye (see text for further details). (A) Right eye of XM28; (B) left eye of XM28; (C) right eye of XP19; (D) left eye of XP19. Left and right eyes were sectioned at different orientations. (Results of the analysis of mid-sections of eyes from chimaeras XM28 and XP19 are shown in Table 3 and photographs of the intact eyes at the time of dissection are shown in Fig. 7.) cor, cornea; on, optic nerve. Numbered arrows indicate equivalent regions on both forms of reconstruction. The arrows and the words 'Inside' and 'Outside' indicate matching edges of the planar and annular reconstruction.

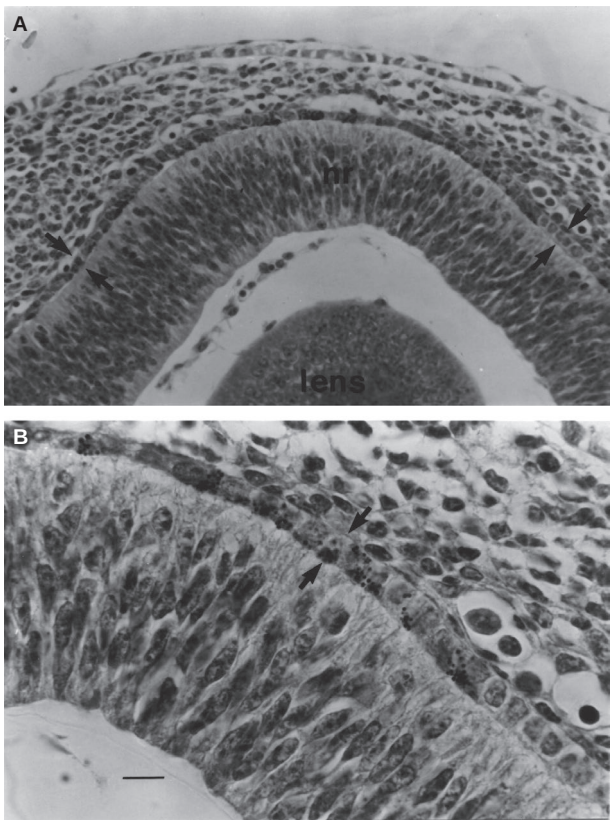

Fig. 9 Histological sections of eye from E12.5 fetal chimaera showing pigmented patches in the RPE (arrows). (A) Low power view (nr = neural retina); (B) high power view; scale bar: 10 μm.

the RPEs of several E12.5 fetal chimaeras show evidence of discontinuous radial clusters of pigmented cells that probably represent descendent clones. This is clearest in the planar reconstructions of right eyes from a series of 'latitudinal' semi-serial sections (Fig. 8A,C) where clusters of pigmented cells appear to radiate from the proximal RPE at the top of the diagram (labelled 'Inside').

One-dimensional analysis of patch lengths in the RPE of mouse chimaeras

The lengths of pigmented and albino RPE patches in sections of fetal and adult chimaeric eyes (Figs 9 and 6B) were measured and compared (Tables 3 and 4). For both fetal and adult chimaeras the corrected mean patch length and the median were numerically similar when p was low but not when p was high. For fetal eyes (Table 3) the corrected mean pigmented patch length was 10.6 μm ($\sim$1.1 cells), whereas the median pigmented patch length was 59.8 μm ($\sim$6.4 cells). However, if the albino patches were measured instead of the pigmented ones when the RPE was more than 50% pigmented, the median patch length (minor component) was reduced to 11.0 μm ($\sim$1.2 cells). Paired *t*-tests also showed no significant difference between the corrected mean pigmented patch length and the median (minor component) patch length for either the left eyes ($P = 0.084$) or the right eyes ($P = 0.195$).

Similarly, for adult eyes (Table 4) the corrected mean pigmented patch length was 44.1 μm ($\sim$3.1 cells) compared to the median (pigmented) patch length of 338.2 μm ($\sim$23.5 cells) and median (minor component) patch length of 43.1 μm ($\sim$3.0 cells). The adult chimaeras used in this study were all unbalanced (either pigmented or albino cells predominated). Paired *t*-tests also showed no significant difference between the corrected mean pigmented patch length and the median (minor component) patch length for either the left eyes ($P = 0.34$) or the right eyes ($P = 0.70$).

These data show that fetal and adult corrected mean patch lengths were significantly different but comparisons between left and right eyes that were sectioned in different planes (Fig. 10) revealed no significant differences in patch lengths. Paired *t*-tests comparing left and right eyes revealed no differences in corrected mean pigmented patch length for either fetal ($P = 0.19$) or adult ($P = 0.96$) eyes. Similarly, there was no difference in median (minor component) patch length between left and right eyes for either fetal ($P = 0.87$) or adult ($P = 0.53$) eyes.

One-dimensional analysis of two-dimensional distribution of patches in the RPE of mouse chimaeras

Although comparisons between eyes sectioned in different planes revealed no significant differences in either the median (minor component) or corrected mean patch lengths in fetal or adult eyes, there is evidence from two-dimensional observations that stripes do exist. RPEs of many adult chimaeras have discontinuous radial clusters of pigmented cells (putative descendent clones) with distal radial patches (Fig. 6A). Also the planar reconstructions of RPEs from at least two fetal chimaeric eyes (right eyes of chimaeras XM28 and XP19) showed discontinuous radial clusters of pigmented cells (Fig. 8A,C).

The computer simulations showed that comparisons of the variance of the percentage of pigmented cells between pairs of perpendicular sections is more likely to detect stripes than comparisons of the median or corrected mean patch lengths. Variation in the percentage of pigmented cells in sections cut in different planes (Fig. 10) was compared as the variance and the percentage coefficient of variation (%CV). For fetal eyes there was no significant difference in either the variance ($P = 0.16$) or the %CV ($P = 0.23$) of the percentage of pigment between eyes cut in different planes (Table 5) but for adults there were significant differences between planes of section for both the variance ($P = 0.019$) and the %CV ($P = 0.044$). In each case the percentage of pigment in sections cut in a longitudinal plane was more variable than in those cut in a latitudinal

Table 3 Comparison of corrected mean and median patch length in the retinal pigment epithelium (RPE) of E12.5 fetal chimaeras.

			Summary statistics of patch length in μm† (mean of all sections)			
Fetal chimaera	No. of sections analysed	Mean % pigment	Corrected mean (pigmented patches)	Median (pigmented)	Median (albino)	Median (minor component)
Right eyes (sectioned in 'latitudinal' plane)						
XM 28	11	5.4	11.3	10.0	199.9	10.0
CA 9*	11	9.9	9.0	8.6	68.1	8.6
XP 19	11	13.8	11.0	9.6	47.7	9.6
CA 15*	11	41.1	10.6	13.3	17.1	13.3
CA 5*	11	52.9	10.5	15.2	15.6	15.6
CA 7	11	93.1	10.9	48.3	10.4	10.4
CA 3	11	97.8	8.9	473.0	8.8	8.8
Left eyes (sectioned in 'longitudinal' plane)						
XM 28	11	4.4	11.6	10.9	164.8	10.9
CA 9*	11	9.6	8.5	8.9	46.3	8.9
XP 19	11	18.3	13.0	12.0	46.1	12.0
CA 15*	11	30.3	10.6	11.3	20.3	11.3
CA 5*	11	77.3	10.2	32.6	10.6	10.6
CA 7	11	90.6	13.0	95.8	13.6	13.6
CA 3	11	92.5	9.4	87.2	9.7	9.7
Right Mean ± SEM		44.8 ± 14.6	10.3 ± 0.4	82.6 ± 65.3	52.5 ± 25.9	10.9 ± 1.0
Left Mean ± SEM		46.1 ± 14.8	10.9 ± 0.7	37.0 ± 14.4	44.5 ± 20.9	11.0 ± 0.6
Right % CV		86.2	9.5	209.2	130.8	23.9
Left %CV		84.9	16.0	103.4	124.4	13.8
Correlation (*P*)‡			NS	0.0002	<0.0001	NS

*$-/-\leftrightarrow Tg/-$ genotype combination; others were non-transgenic, $-/-\leftrightarrow-/-$.
†Estimated mean RPE cell length at E12.5 = 9.0–9.5 μm (West, 1976a).
‡*P*-value for the median (minor component) is for Kendall's correlation with the % of the minority cell population (pigmented or albino). Others are for correlations with the % pigmented cells. NS = not significant ($P \geq 0.05$).
%CV, % coefficient of variation.

plane (Table 6), which is consistent with the longitudinal radial stripes observed more directly in two dimensions (Figs 6A and 8A,C).

Discussion

The computer simulations of random and clumped arrays predicted that the median patch length of the minority cell population and the corrected mean patch length would provide numerically similar estimates of the coherent clone length in chimaeric tissues and so both would distinguish between random and clumped patterns. This was confirmed by studies of chimaeric RPEs. The corrected mean patch length and the median were numerically similar when p was low, but the median increased when p was high. This similarity has already been demonstrated for eyes of unbalanced E12.5 fetal chimaeras, where the corrected mean patch length is only equivalent to a single cell (West et al. 1997). The demonstration that this was also true for adult eyes showed that the two measures are numerically similar even when many of the coherent clones comprise more cells. This study also showed that the median patch length of the minority cell population was applicable to balanced as well as unbalanced chimaeras. In fact, for simulated striped arrays the median patch length of the minority cell population appeared to be superior to the corrected mean patch length.

Comparison between results for fetal and adult chimaeras also showed that the corrected mean patch length increased from 10.6 to 44.1 μm, thus confirming that this analysis can distinguish different degrees of cell mixing. This increase is equivalent to a growth in patch size from 1.1 to 3.1 cells per corrected mean patch length (or 1.2–9.6 cells per corrected mean patch area) and is in good agreement with a previous estimate (West, 1976a). The median patch length of the minority cell population increased by an almost identical amount from 10.9 to 43.0 μm (from 1.2 to 3.0 cell lengths). However, these increases in the corrected mean and median patch sizes do not reflect a uniform growth of all the coherent clones. From observations of two-dimensional patterns it is clear that the coherent clones in the adult RPE are heterogeneous in size and shape (Schmidt et al. 1986) and also appear to be clustered into descendent clones that form radial sectors (Sanyal & Zeil-

Table 4 Comparison of corrected mean and median patch lengths in the RPE of adult chimaeras.

			Summary statistics of patch length in μm† (Mean of N sections)			
Adult chimaera	No. of sections analysed (N)	Mean % pigment	Corrected mean (pigmented patches)	Median (pigmented)	Median (albino)	Median (minor component)
Left eyes (sectioned in 'latitudinal' plane)						
AdCA 17*	9	14.0	47.5	40.3	232.5	40.3
AdCA 18*	8	31.0	52.1	52.5	96.5	52.5
AdCA 29**	11	86.8	39.4	238.6	39.9	39.9
AdCA 30*	9	81.7	38.3	139.9	37.3	37.3
AdCA 21**	9	73.1	35.4	102.9	31.4	31.4
AdCA 20**	9	87.0	45.9	172.2	41.7	41.7
AdCA 19*	10	92.2	53.5	430.5	46.0	46.0
AdCA 23*	8	92.4	44.1	370.2	53.4	53.4
AdCA 24*	8	96.6	40.5	1424.8	38.8	38.8
Right eyes (sectioned in 'longitudinal' plane)						
AdCA 17*	14	24.0	48.4	43.5	120.5	43.5
AdCA 18*	15	32.4	49.5	54.0	47.5	54.0
AdCA 29**	16	75.6	44.3	127.3	42.3	42.3
AdCA 30*	13	66.4	45.1	87.2	44.6	44.6
AdCA 21**	10	87.0	39.7	210.0	38.7	38.7
AdCA 20**	15	87.5	45.1	312.6	47.4	47.4
AdCA 19*	15	93.4	43.1	836.0	44.9	44.9
AdCA 23*	15	96.9	45.2	671.1	40.2	40.2
AdCA 24*	14	95.1	37.2	773.7	38.1	38.1
Left Mean ± SEM		72.8 ± 9.9	44.1 ± 2.1	330.2 ± 144.0	68.6 ± 21.5	42.4 ± 2.4
Right Mean ± SEM		73.1 ± 9.1	44.2 ± 1.3	346.1 ± 108.0	51.6 ± 8.7	43.7 ± 1.6
Left % CV		40.7	14.2	130.8	93.9	16.9
Right %CV		37.4	8.7	93.6	50.6	11.2
Correlation (*P*)‡			NS	<0.0001	NS	NS

*$-/-\leftrightarrow Tg/-$ genotype combination; ** $-/-\leftrightarrow Tg/Tg$ genotype combination.
†Estimated mean adult RPE cell length = 14.4 μm (West, 1976a).
‡*P*-value for the median (minor component) is for Kendall's correlation with the % of the minority cell population (pigmented or albino). Others are for correlations with the % pigmented cells. NS = not significant ($P \geq 0.05$).

maker, 1977; West, 1978). The coherent clones in the proximal region are produced during fetal development when cell mixing is high (Bodenstein & Sidman, 1987a) and are mostly individual cells (Schmidt et al. 1986). Larger, radially elongated coherent clones are produced in the distal region at a later stage when cell mixing is reduced and proliferation is largely restricted to the edge of the tissue (Bodenstein & Sidman, 1987a,b). Also, the corrected mean patch length may be an imprecise estimate of the coherent clone length so the numerical values probably have more statistical than biological significance and should be used only for comparative studies, as illustrated here. Although the

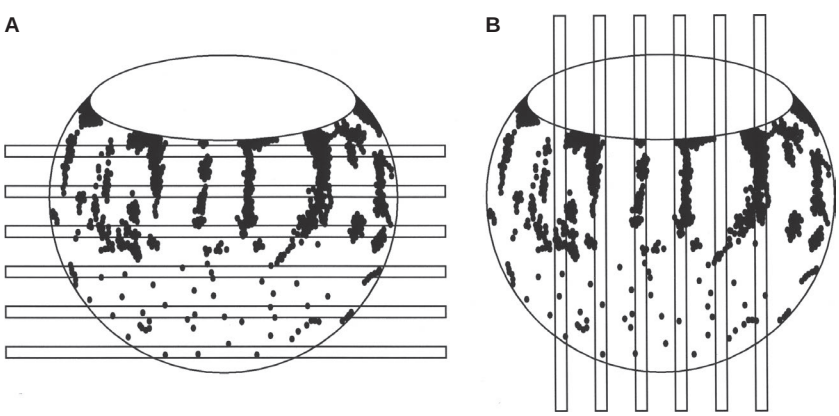

Fig. 10 Diagram showing expected relationship between planes of sections and radial stripes in the distal retinal pigment epithelium (RPE). The RPE is orientated so the proximal-distal axis is vertical (the proximal region is at the bottom). (A) Horizontal ('latitudinal') sections are orientated perpendicular to the stripes. (B) Vertical ('longitudinal') sections near the middle of the RPE are orientated nearly parallel to the stripes but because the RPE is cup-shaped, the more peripheral sections are not completely parallel to the stripes.

Table 5 Comparison of variability in percentage pigment in the RPE of E12.5 fetal chimaeric eyes sectioned in different planes.

	Variability in % pigment among sections analysed			
	Variance		% Coefficient of variation	
Fetal chimaera	Right eye ('latitudinal')	Left eye ('longitudinal')	Right eye ('latitudinal')	Left eye ('longitudinal')
XM 28	4.99	2.91	41.68	39.04
CA 9*	8.94	15.77	30.32	41.37
XP 19	17.13	36.40	30.08	32.99
CA 15*	17.08	25.45	10.06	16.65
CA 5*	11.61	4.43	6.44	2.72
CA 7	7.24	6.75	2.89	2.87
CA 3	2.29	30.20	1.55	5.94
Mean ± SEM	9.90 ± 2.16	17.42 ± 5.08	17.57 ± 6.08	20.23 ± 6.53

*−/−↔*Tg*/− genotype combination; others were non-transgenic, −/−↔−/−.
Paired *t*-tests showed no significant difference between eyes for either the variance of the percentage pigment ($P = 0.16$) or the percentage coefficient of variation ($P = 0.23$).

Table 6 Comparison of variability in percentage pigment in the RPE of adult chimaeric eyes sectioned in different planes.

	Variability in % pigment among sections analysed			
	Variance		% Coefficient of variation	
Adult chimaera	Left eye ('latitudinal')	Right eye ('longitudinal')	Left eye ('latitudinal')	Right eye ('longitudinal')
AdCA 17*	12.27	61.48	25.11	32.62
AdCA 18*	11.81	169.44	11.09	40.21
AdCA 29**	14.32	59.65	4.36	10.22
AdCA 30*	24.20	84.27	6.02	13.83
AdCA 21**	11.59	47.25	4.66	7.90
AdCA 20**	5.59	21.09	2.72	5.25
AdCA 19*	5.99	33.31	2.65	6.18
AdCA 23*	7.03	10.07	2.87	3.28
AdCA 24*	2.27	13.45	1.56	3.86
Mean ± SEM	10.6 ± 2.1	55.6 ± 16.4	6.8 ± 2.5	13.7 ± 4.5

*−/−↔*Tg*/− genotype combination; **−/−↔*Tg*/*Tg* genotype combination.
Paired *t*-tests showed that the variance of the percentage pigment was significantly greater for the right eyes, sectioned in the 'longitudinal plane' ($P = 0.019$), as was the corresponding difference in the percentage coefficient of variation ($P = 0.044$).

computer-generated clumped arrays simulated chimaeric tissues with a uniform distribution of symmetrical coherent clones of 2×2 or 4×4 cells which is simpler than the pattern seen in the adult RPE, both the median patch length of the minority cell population and the corrected mean patch length identified differences in cell distributions between fetal and adult RPEs as well as between different types of simulated arrays.

The second prediction made by the analysis of simulated arrays was that it would be possible to identify two-dimensional striped patterns in chimaeric tissues by comparing the variances of the percentage of pigmented cells in two perpendicular series of sections. This was borne out by the significantly higher variance in percentage of pigmented RPE cells among sections of adult chimaeric eyes cut in the 'longitudinal' plane than the 'latitudinal' plane. This may reflect both the radial clusters of putative descendent clones and the radially elongated patches in the distal RPE. This approach is presumably quite robust because stripes are discontinuous and the curvature of the eye means that the 'longitudinal' sections will not all be aligned parallel to the stripes (Fig. 10). Nevertheless, the radial clusters of putative descendent clones that were apparent in some two-dimensional reconstructions of semi-serial sections of fetal

eyes (Fig. 8A,C) were not identified by this approach. Presumably the absence of the distal radially elongated patches adds to problems of the fragmented nature of the putative descendent clone and the curved shape of the RPE to make the radial pattern more difficult to detect in the fetal RPE than the adult.

The approach to one-dimensional spatial analysis of two-dimensional patterns could be extended to other chimaeric or mosaic tissues either by cutting separate representative samples in perpendicular planes or by re-orientating the wax block on the chuck of the microtome to cut two perpendicular sets of sections from the same sample (e.g. West, 1976a). However, comparing results from paired perpendicular transects will not reveal all types of striped patterns and other strategies may have to be devised. As noted in the Introduction, Boland & Gosden (1994) compared radial and concentric, circumferential transects to identify suspected radial patterns in two-dimensional sections of three-dimensional ovarian follicles.

A previous analysis of patterns in mouse chimaeras (Schmidt et al. 1985) used the Greig-Smith analysis of variance, which is a two-dimensional method using different sized quadrats or grids that was developed for ecological research (Greig-Smith, 1952). The one-dimensional methods described here may also be relevant to other fields, including ecological studies using one-dimensional transect lines to sample plants or animals in habitats that can be treated as two-dimensional. For example, sightings of whales from a ship can be plotted on a one-dimensional transect line, representing the course steered by the ship. Various methods have been proposed to use such data to estimate both whale numbers and their spatial distributions (Cowling, 1998; Niemi & Fernandez, 2010), and the one-dimensional methods we describe here may also be useful.

This study has demonstrated that one-dimensional methods of analysis can identify two types of non-random two-dimensional mosaic patterns (clumps and stripes) both in simulated mosaic arrays and chimaeric tissues without full reconstruction of the two-dimensional structure from serial sections. Both the corrected mean patch length and the median patch length of the minority cell population accurately distinguished different extents of cell mixing in both unbalanced and balanced arrays. However, each of these summary statistics has different advantages and disadvantages so it would be worth using them both in future studies where estimates of the coherent clone size are required to compare the extent of cell mixing in different groups of mosaic or chimaeric tissues.

Acknowledgements

We thank Jean Flockhart for expert technical assistance, Sheila MacPherson and Mike Millar for preparing the plastic sections, Denis Doogan, Maureen Ross and Jim Macdonald for mouse husbandry and Tom McFetters, Ted Pinner and Ronnie Grant for help in preparing the figures. We are grateful to Prof. Jamie Davies for facilitating access to resources and staff time for the computer simulations. B.A.H. was supported by the Wellcome Trust (grants 039613 and 043031 to J.D.W.) and M.U. was supported by a grant from EU programme FP6 036-97-2 (KidStem), awarded to Jamie Davies.

References

Bodenstein L (1986) A dynamic simulation model of tissue growth and cell patterning. *Cell Differ* **19**, 19–33.

Bodenstein L, Sidman RL (1987a) Growth and development of the mouse retinal pigment epithelium. I. Cell and tissue morphometrics and topography of mitotic activity. *Dev Biol* **121**, 192–204.

Bodenstein L, Sidman RL (1987b) Growth and development of the mouse retinal pigment epithelium. II. Cell patterning in experimental chimeras and mosaics. *Dev Biol* **121**, 205–219.

Boland NI, Gosden RG (1994) Clonal analysis of chimeric mouse ovaries using DNA in-situ hybridization. *J Reprod Fertil* **100**, 203–210.

Collinson JM, Morris L, Reid AI, et al. (2002) Clonal analysis of patterns of growth, stem cell activity, and cell movement during the development and maintenance of the murine corneal epithelium. *Dev Dyn* **224**, 432–440.

Collinson JM, Chanas SA, Hill RE, et al. (2004) Corneal development, limbal stem cell function, and corneal epithelial cell migration in the *Pax6*$^{+/-}$ mouse. *Invest Ophthalmol Vis Sci* **45**, 1101–1108.

Cowling A (1998) Spatial methods for line transect surveys. *Biometrics* **54**, 828–839.

Greig-Smith P (1952) The use of random and contiguous quadrats in the study of the structure of plant communities. *Ann Bot* **16**, 293–316.

Kerr JB, Sharpe RM (1985) Stimulatory effect of follicle-stimulating hormone on rat Leydig cells – A morphometric and ultrastructural study. *Cell Tissue Res* **239**, 405–415.

Lo C (1986) Localization of low abundance DNA sequences in tissue sections by in situ hybridization. *J Cell Sci* **81**, 143–162.

Mintz B (1971) The clonal basis of mammalian differentiation. In: *Control Mechanisms of Growth and Differentiation, Symposia of the Society for Experimental Biology*. (eds Davies DD, Balls M), pp. 345–370. London: Cambridge University Press.

Mintz B, Gearhart JD, Guymont AG (1973) Phytohemagglutinin-mediated blastomere aggregation and development of allophenic mice. *Dev Biol* **31**, 195–199.

Mort RL (2009) Quantitative analysis of patch patterns in mosaic tissues with ClonalTools software. *J Anat* **215**, 698–704.

Mort RL, Ramaesh T, Kleinjan DA, et al. (2009) Mosaic analysis of stem cell function and wound healing in the mouse corneal epithelium. *BMC Dev Biol* **9**, 4.

Mullen RJ (1977) Site of *pcd* gene action and Purkinje cell mosaicism in the cerebella of chimaeric mice. *Nature* **270**, 245–247.

Nesbitt MN (1971) X-chromosome inactivation mosaicism in the mouse. *Dev Biol* **26**, 252–263.

Niemi A, Fernandez C (2010) Bayesian spatial point process modeling of line transect data. *J Agr Biol Env Stat* **15**, 327–345.

Oster-Granite ML, Gearhart J (1981) Cell lineage analysis of cerebellar Purkinje cells in mouse chimeras. *Dev Biol* **85**, 199–208.

Roach SA (1968) *The Theory of Random Clumping*. London: Methuen.

Sanyal S, Zeilmaker GH (1977) Cell lineage in retinal development of mice studied in experimental chimaeras. *Nature* **265**, 731–733.

Schmidt GH, Wilkinson MM, Ponder BAJ (1985) Detection and characterization of spatial pattern in chimaeric tissue. *J Embryol Exp Morphol* **88**, 219–230.

Schmidt GH, Wilkinson MM, Ponder BAJ (1986) Non-random spatial arrangement of clone sizes in chimaeric retinal pigment epithelium. *J Embryol Exp Morphol* **91**, 197–208.

Tarkowski AK (1961) Mouse chimaeras developed from fused eggs. *Nature* **190**, 857–860.

Tarkowski AK (1964) Patterns of pigmentation in experimentally produced mouse chimaeras. *J Embryol Exp Morphol* **12**, 575–585.

West JD (1975) A theoretical approach to the relation between patch size and clone size in chimaeric tissue. *J Theor Biol* **50**, 153–160.

West JD (1976a) Clonal development of the retinal epithelium in mouse chimaeras and X-inactivation mosaics. *J Embryol Exp Morphol* **35**, 445–461.

West JD (1976b) Patches in the livers of chimaeric mice. *J Embryol Exp Morphol* **36**, 151–161.

West JD (1978) Analysis of clonal growth using chimaeras and mosaics. In: *Development in Mammals* (ed. Johnson MH), pp. 413–460. Amsterdam: Elsevier.

West JD (1999) Insights into development and genetics from mouse chimeras. *Curr Top Dev Biol* **44**, 21–66.

West JD, Flockhart JH (1994) Genotypically unbalanced diploid↔diploid foetal mouse chimaeras: possible relevance to human confined mosaicism. *Genet Res* **63**, 87–99.

West JD, Hodson BA, Keighren MA (1997) Quantitative and spatial information on the composition of chimaeric fetal mouse eyes from single histological sections. *Develop Growth Differ* **39**, 305–317.